Using DEM hindcasting to determine screw pile performance for practical design

Sharif, Yaseen; Brown, Michael; Ciantia, Matteo; Lutenegger, Alan; Kumar, Pavan; Patra, Shantanu

Published in:
Geotechnique Letters

DOI:
10.1680/jgele.21.00071

Publication date:
2021

Géotechnique Letters

USING DEM HINDCASTING TO DETERMINE SCREW PILE PERFORMANCE FOR PRACTICAL DESIGN

GELE-2021-071-R2 | Letter

Submitted on: 19-08-21

Submitted by: Yaseen Sharif, Michael John Brown, Matteo Ciantia, Alan Lutenegger, Pavan Kumar, Shantanu Patra, Sumanta Haldar

Keywords: GEOTECHNICAL ENGINEERING, PILES & PILING, COMPUTATIONAL MECHANICS

RIVER VALLEY
TECHNOLOGIES

Date of 1st submission: 17/06/2021

Date of resubmission after 1st review: 19/08/2021

Title: USING DEM HINDCASTING TO DETERMINE SCREW PILE PERFORMANCE FOR PRACTICAL DESIGN

Yaseen U. Sharif, MEng

*Corresponding author: Yaseen Sharif, Research Student, Civil Engineering, Fulton Building, University of Dundee, Dundee, DD1 4HN

ORCID: 0000-0002-3620-7500
Email: y.u.sharif@dundee.ac.uk

Prof Michael J Brown, BEng (Hons), PhD, GMICE
Professor of Geotechnical Engineering, School of Science and Engineering, University of Dundee, Fulton Building
Dundee DD1 4HN UK

ORCID: 0000-0001-6770-4836
Email: m.j.z.brown@dundee.ac.uk

Dr Matteo O Ciantia
Senior Lecturer, School of Science and Engineering, University of Dundee, Fulton Building
Dundee DD1 4HN UK

ORCID: 0000-0003-1897-4471
Email: m.o.ciantia@dundee.ac.uk

Alan J Lutenegger, BSc, MSc, PhD
Professor, Department of Civil & Environmental Engineering, University of Massachusetts
Amherst, Ma. USA 01003

ORCID: 0000-0002-6574-5957
Email: aluteneg@engin.umass.edu, lutenegg@ecs.umass.edu

P.V. Pavan Kumar,
Research Scholar, Department of Civil Engineering, Indian Institute of Technology, Bhubaneswar-752050

ORCID: 0000-0003-0411-7698
Email: pvk11@iitbbs.ac.in

Shantanu Patra
Assistant Professor, Department of Civil Engineering, Indian Institute of Technology, Bhubaneswar-752050

ORCID: 0000-0001-8827-8194
Email: shantanupatra@iitbbs.ac.in

Sumanta Haldar
Associate Professor, Department of Civil Engineering, Indian Institute of Technology, Bhubaneswar-752050

ORCID: 0000-0002-8575-8317
Email: sumanta@iitbbs.ac.in

Word count: 3080

Number of Figures:8

Number of Tables:2

USING DEM HINDCASTING TO DETERMINE SCREW PILE PERFORMANCE FOR PRACTICAL DESIGN

Yaseen Sharif, Michael J Brown, Matteo O Ciantia
School of Science and Engineering, University of Dundee, Fulton Building
Dundee DD1 4HN UK

Alan J Lutenegger
Department of Civil & Environmental Engineering, University of Massachusetts Amherst, Ma. USA 01003

P.V. Pavan Kumar, Shantanu Patra, Sumanta Haldar
Department of Civil Engineering, Indian Institute of Technology, Bhubaneswar-752050

Abstract

Screw piles have been used to support a variety of structures due to their ease of installation and high axial capacity. Recently screw piles have been proposed as an alternative foundation solution for offshore renewable structures owing to their quiet or silent installation. Due to their variable geometry, design and prediction of installation requirements and its effect on in service capacity may be challenging. In this paper, the discrete element method is used to numerically recreate a series of onshore field tests. The aim of the paper is to investigate the ability of DEM to be used as a practical design tool for the design and deployment of screw piles. In this case study, the effect of the geometric helix pitch on the installation torque and tensile capacity of screw piles installed into sand is investigated. DEM results show that the geometric pitch of a screw pile appears to have little effect on the installation torque. The results show that DEM has the potential to be used as a practical design procedure for complex foundation installation where the simulation needs to capture installation effects.

Keywords: Geotechnical engineering, Piles & piling, Computational mechanics

Introduction

A screw pile consists of a central steel shaft, with one or more helical plates welded to it. Screw piles are generally installed by the application of a vertical compressive force (“crowd force”) and torque. They may be considered as a “silent” or quiet pile as they do not require hammer installation as per driven piles (Huisman, 2019). They are able to mobilise significant axial resistance as the helix acts as an embedded plate and have been used for many different structures, including buildings, bridges, railway gantries and electricity pylons (Lutenegger, 2011a). Once the geometry for a specific application has been decided there is then the need to check the installation requirements and in-service performance. This is normally done based upon empirical approaches that do not directly consider the effects of installation and assume perfect or pitch matched installation where there may be little control of this in the field.

The most common approach to verify the ultimate capacity of a screw pile is the empirical torque correlation factor (K_t). The K_t method links the installation torque (T) to the ultimate tensile capacity (Q_t) (equation 1) and does not account for any variation in crowd or vertical force required during installation (Hoyt and Clemence 1989). The value of K_t is normally calculated based upon the diameter of the pile core and is considered to be a fixed value irrespective of pile geometry, soil, or installation approach (e.g. over flighting (AR < 1) or under flighting (AR > 1)).

$$Q_t = TK_t \tag{1}$$

3

Perko (2009) proposed an empirical relationship for K_t based upon the shaft diameter (D_c). Although a single value is determined from equation 2, it should be noted that considerable scatter is present in the original data set.

$$K_t = 22.285{D_c}^{-0.9198} \tag{2}$$

The validity of using K_t, has previously been questioned as it fails to consider many additional factors that contribute to the installation torque and ultimate capacity (Lutenegger, 2013; Davidson *et al.*, 2020; Cerfontaine *et al.*, 2021; Sharif *et al.*, 2021). Using a series of field tests, Lutenegger (2013) showed that piles with the same shaft and helix diameters (D_h) but different geometric pitches (3, 4 and 6 inches or 76.2, 101.6 and 152.4 mm) result in different values of K_t. Although, the K_t method is commonly used, previous studies have shown that it may not be a reliable tool (some codes stating that it should actually not be used in design e.g. BS8004:2015).

In this paper DEM is used to simulate insitu CPT testing and full screw pile installation and loading. The discrete element method (DEM), which naturally allow granular behaviour to arise through the use of very simple contact models, has gained much relevance in geomechanics since originally proposed (Cundall and Strack, 1979). To date widespread use of DEM has been limited in a commercial setting due to the computational time required but recent developments have reduced this time including faster sample preparation (Ciantia *et al.*, 2018) coupled with lower cost higher performance computing. This has resulted in an increase in DEM application to analyse boundary value problems at model (Boschi *et al.*, 2020; Nguyen *et al.*, 2020; Zhang *et al.*, 2021) and field scale (Boon *et al.*, 2014; Previtali *et al.*, 2021).

The aim of this paper is to assess whether *DEM* could be used as a design tool to predict real performance and then optimise the design of a screw pile. This involves using real CPT data to create a DEM soil bed to an appropriate relative density to match the soil encountered in the field. A DEM simulation of the insitu CPT was then used to validate the appropriateness of the soil bed created and the ability to replicate the "real" soil profile into which models of the real screw piles were installed and loaded. The process was undertaken in the form of a Class C prediction (Lambe, 1973) without the use of any refinement of the approach (to simulate commercial time frames). The field data includes screw piles with helices of different pitch (but the same diameter) which allowed additional commentary on assumptions with respect to K_t and the effect of pitch variation on pile performance (Lutenegger 2013). This study highlights the practical use of DEM as a design tool for large deformation problems and identifies where further refinement and improvement is required.

Methodology

To recreate the stratigraphy of the soil in the field testing in DEM soil bed data was obtained from cone penetration testing (CPT) at the Agricultural Farm site, University of Massachusetts, Amherst (Lutenegger, 2011b) (Figure 1a). To recreate a simple or averaged soil profile the CPT cone resistance (q_c) was used to determine relative density (Jamiolkowshi *et al.*, 1985) (Figure 1b).

Using the calculated relative density from the field CPT (Figure 1b), a simplified soil profile was created, consisting of three layers of sand each having a different relative density. The targeted relative densities were then used to calculate target voids ratios for each soil layer during the bed formation process. To reduce complexity, the clay layer 1 m below the required helix depth (3 m) was modelled as a continuation of the dense sand layer (above). The effect on the results of this assumption is thought to be limited, as the pile penetrates in the upper sand layers and only tensile loading was applied. A DEM representation of each layer was then created using parameters of a known sand which has previously been calibrated against laboratory triaxial tests (Table 1) (Sharif *et al.*, 2019a). To create the soil layers the radius expansion method was used along with the periodic cell replication method (Ciantia *et al.*, 2018).

The sand modelled in the simulations is based upon the properties of HST95, which is a medium to fine well graded sand (Al-Defae et al., 2013; Lauder et al., 2013). These parameters were not specific to the field study site as it was felt this may not be available in a commercial setting. In absence of this, it may be possible to tune the soil contact model to suit the observed CPT data but this would involve a trial and error process for sample formation which as shown in Table 3 can take considerable time. To model the geometry of the screw pile, rigid boundaries, with the interface properties previously calibrated and validated against centrifuge tests by Sharif et al. (2019a) were used. The geometries match the piles used in the field tests, the main geometric controls were kept constant, e.g. the helix and shaft diameter, whilst the helix pitch was varied. The final embedment depth of the piles was 3m below ground level (BGL) (Figure 2). The shaft of the screw piles were modelled as being artificially plugged due to the size of the particles in relation to the shaft diameter. This is similar to the approach adopted in small physical modelling where plugging cannot be adequately scaled due to particle size effects (Davidson *et al.*, 2020). During the field test the screw piles had an open central core resulting in an average plug length ratio of 0.15 indicating that they plugged early on in the installation process and therefore effectively behaved as plugged piles. Thus the approach adopted in the DEM modelling is effectively the same as that encountered in the field. The location of the screw pile installations compared to the CPT can be seen in Figure 3. The screw piles were installed at a maximum distance of 6.7m from the location of the CPT.

To reduce the run time of the simulations the particle refinement method (McDowell *et al.*, 2012) was used in the soil bed formation (Figure 4). This process uses scaling of the particle size distribution (PSD) in the central region of the soil bed, and an increasingly larger *PSD* scaling in regions further away (Sharif *et al.*, 2019b). This method allows for a smaller number of total particles to be present within the soil model without losing the resolution of results in the region of most interest, similar to mesh refinement in finite element modelling. To ensure that multiple particles are able to pass through the opening of the smallest helix pitch (3 inch or 76.2 mm) the scaling of the *PSD* in the central zone was limited to 120 (largest particle diameter of 25.5 mm), which typically results in an average of 30 particles passing through the opening of the 3-inch (76.2 mm) helix pitch (Figure 4c). The properties of the contact model for each soil layer were the same, allowing for the total number of particles to be significantly reduced (Table 2). This ultimately reduces the run time, while maintaining the precision of particle scaling.

Once the bed was created a 36mm diameter virtual CPT was conducted (the same diameter as the one used in the site investigation of the AGFarm site) in the soil bed and compared to the field data to validate the approach (Figure 1). The results of the DEM CPT generally match those of the field test although the DEM underestimates the cone resistance of the sand near the surface and the CPT resistance at 3m BGL. This is thought to be due to loosening of the dense soil layer, when the individual layers are combined during bed creation. As layers are created in isolation, the contact forces at the interface between layers are only formed when combined. The contact forces may become very large, resulting in the individual particles moving away from one another in attempt to equilibrate. This results in a loosening of the dense layer and densification of the medium dense layer above. This may suggest a need to form denser layers to offset this loosening during combination. With further refinement it would be possible to improve the match to the field CPT results but as this was an experiment in seeing how commercially applicable the approach is, this was not done here.

To model installation of each screw pile, the advancement ratio (AR) (Sharif *et al.*, 2021), defined as the displacement for a single rotation divided by the geometric pitch of the screw pile, measured in the field tests was replicated (Figure 5). From the study of Sharif *et al* (2021) it is known that the advancement ratio of the pile has a significant effect on the axial capacity of the screw pile. Thus, the advancement ratio from the field tests were replicated in the DEM simulations. Once the pile reached the required depth, the pile was unloaded, and an uplift (tensile) test conducted.

To assess the practicality of using DEM commercially the time taken for each operation is shown in Table 3. All simulations were conducted using an Intel Xeon E5-2630v3 with 32Gb of RAM and PFC3D 5.0.39 (Itasca Consulting Group, 2016)

Results and discussion

The installation torque, uplift capacity and K_t values for each pile field test and comparative DEM simulation can be seen in Figure 6 to Figure 8. Compressive installation force (crowd force) are not typically recorded in practice and were not recorded during field test installation and therefore cannot be compared with the results of the DEM simulations.

The comparison of the installation torque between the DEM results and those of the field tests are generally consistent (Figure 6). The DEM results for the 4-inch and 6-inch helices are very close to the field tests, while the numerical prediction overestimates the torque for the 3-inch geometry. The difference between the DEM and field results could be explained by the heterogeneity of the soil profile in the field, and the average representation of the soil layers in DEM, that can be seen in Figure 6. This could be addressed by further evolution of the soil bed (i.e. accounting for the loosening during sample formation mentioned previously), but it highlights that DEM could be used to predict installation requirements for piles of different geometry. Comparison between the uplift capacity from DEM and field tests shows a similar trend (Figure 7). The stiffness is very consistent, although the ultimate capacity is under predicted (typically a 12 % decrease at z/D_h = 0.1) although a very similar trend with increasing helix pitch is seen. This is thought to be due to the differences in the field between the CPT and pile locations and how well the DEM soil bed matched reality. The latter may have a stronger effect as the pile helices are installed where the DEM CPT simulation results in the greatest "averaging" compared to that measured in the field (Figure 1a at a depth of 2.5 m to 3.2m). In uplift this would seem to be one of the more important regions for careful replication in DEM and with hindsight could have been split into sub layers in the DEM bed.

When assessing the effect of the helix pitch on the installation torque, it appears insensitive to the helix pitch (within the range tested) with only some limited variation observed in the field study. A potential reason for this variation could be the difference in advancement ratio (AR) (Figure 5) and how well this was controlled during field installation. Field testing undertaken by Richards *et al*., (2019) also showed limited effects of helix pitch on installation torque for two D_h/D_c (helix diameter to shaft diameter) ratios. In their study the pitch was varied from 100-200mm (approx. 4" to 8"). Further investigation would be required using a single AR to clearly identify the effect of the helix pitch and AR independently.

The ultimate capacity Q_t, defined at z/D_h = 0.1 was used to back calculate the value of K_t for each of the piles (Figure 7). Figure 8 shows the values of K_t for both the DEM and field tests where the values vary considerably. K_t ranges between 24 and 15 for the field tests and 20 and 25 for the DEM results. Variation in the K_t is a result of the difference in pile tensile capacity with the 6-inch (152.4 mm) helix pitch having an 8% increase in capacity compared to the 3-inch (75.2 mm) pile and no increase in installation torque. This is contrary to the assumption that the torque correlation factor should be constant with the shaft diameter and not change with helix pitch or soil conditions. The value of K_t calculated using equation 2 results in a value of 25.3, which is greater than all but one of those found herein and would result in over prediction of pile capacity by up to 18%.

Conclusion

This study uses DEM simulation to hindcast field behaviour to see if CPT data can be used to create an appropriate DEM soil model and then use this to predict field screw pile behaviour. Using CPT tests conducted at a field site, a layered soil bed was created using DEM to match the relative density encountered. This was done without any refinement or evolution of the DEM model to simulate the time pressures of a commercial environment. The numerical simulations were generally able to reproduce the installation torque and uplift capacity recorded from field pile tests. Variations between the field study and the DEM simulations occurred due to the idealised soil profiles and heterogeneity within the field site, although with more time a more realistic DEM soil bed could be prepared.

The results of the DEM simulations suggest that the installation torque is insensitive to helix pitch, however, the uplift capacity may be affected. No definitive trend of how the helix pitch affects ultimate capacity was observed although it appeared to increase for the greatest pitch. As the advancement ratio (AR) varies for each of the piles it is difficult to separate out the effects of the helix pitch and AR. The results do however suggest that there is no single value of K_t for screw piles that have the same shaft diameter but other geometry variations. Further work is required to understand which properties of the screw pile, the soil (e.g. layered soils) and the installation method (e.g. variable AR during installation) effect the installation and in-service behaviour. This work shows that DEM is a powerful simulation technique in the study of large deformation installation and loading processes and that with further refinement could see greater use as a commercially viable design tool.

Acknowledgments

This research is a part of an EPSRC NPIF funded studentship with Roger Bullivant Limited (Grant no. 617 EP/R512473/1). The work is also supported by Scheme for Promotion of Academic and Research Collaboration (SPARC) to allow collaboration between Indian Researchers and other international centres of research and teaching excellence.

References

Boon, C. W., Houlsby, G. T. and Utili, S. (2014) New insights into the 1963 Vajont slide using 2D and 3D distinct-element method analyses, *Geotechnique*, 64(10), pp. 800–816. doi: 10.1680/geot.14.P.041.

Boschi, K., di Prisco, C. G. and Ciantia, M. O. (2020) Micromechanical investigation of grouting in soils, *International Journal of Solids and Structures*, 187. doi: 10.1016/j.ijsolstr.2019.06.013.

British Standards Institute (2015) *BS8004:2015 Code of practice for foundations*. London United Kingdom.

Cerfontaine, B., Brown, M. J., Knappett, J. A., Davidson, C., Sharif, Y. U., Huisman, M. and Ottolini, M. (2021) Control of screw pile installation to optimise performance for offshore energy applications, *Géotechnique (Accepted/ In Press)*.

Ciantia, M. O., Boschi, K., Shire, T. and Emam, S. (2018) Numerical techniques for fast generation of large discrete-element models, *Proceedings of the Institution of Civil Engineers - Engineering and Computational Mechanics*, 171(4), pp. 147–161. doi: 10.1680/jencm.18.00025.

Cundall, P. A. and Strack, O. D. L. (1979) A discrete numerical model for granular assemblies, *Géotechnique*. Thomas Telford Ltd , 29(1), pp. 47–65. doi: 10.1680/geot.1979.29.1.47.

Davidson, C., Brown, M. J., Cerfontaine, B., Knappett, J. A., Brennan, A. J., Al-Baghdadi, T., Augarde, C., Coombs, W., Wang, L., Blake, A., Richards, D. and Ball, Jonathan, D. (2020) Physical modelling to demonstrate the feasibility of screw piles for offshore jacket-supported wind energy structures, *Geotechnique Published online 16/12/2020*. doi: doi.org/10.1680/jgeot.18.P.311.

Hoyt, R. . and Clemence, S. P. (1989) Uplift capacity of helical anchors in soil, in *Proceedings of the 12th International conference on Soil Mechanics and Foundations*. Rio de Janeiro, pp. 1019–1022.

Huisman, M. (2019) Silent Foundation Concept: Helical Piles For Skirt and Pre-piled Jacket Foundations, in Davidson, C. ;, Brown, M. J., Knappett, J. A., Brennan, A. J., Augarde, C. E., Coombs, W. M., Wang, L., Richards, D., White, D. J., and Blake, A. (eds) *International Symposium on Screw Piles for Energy Applications*. Dundee, United Kingdom, pp. 117–118. doi: 10.20933/100001123.

Itasca Consulting Group, I. (2016) PFC 5.0. Minneapolis: Itasca Consulting Group, Inc.

Jamiolkowshi, M., Ladd, C., Germaine, J. . and Lancellotta, R. (1985) New developments in field and laboratory testing of soils, in *Proceedings of the 11th Internaltional conference on Soil Mechanics and Foundation Engineering*. San Fransico, USA: Balkema Pub, Rotterdam, pp. 57–153.

Lambe, T. W. (1973) Predictions in soil engineering, *Geotechnique*, 23(2), pp. 151–202. doi: 10.1680/geot.1973.23.2.151.

Lutenegger (2011a) Historical Development of Iron Screw-Pile Foundations: 1836–1900, *The International Journal for the History of Engineering & Technology*, 81(1), pp. 108–128. doi: 10.1179/175812109x12547332391989.

Lutenegger, A. (2011b) Behavior of multi-helix screw anchors in sand, in *Proceedings of the 14th Pan-American Conference on Geotechnical Engineering*, pp. 1–6.

Lutenegger, A. J. (2013) Factors Affecting Installation Torque and Torque-To-Capacity Correlations for Screw-Piles and Helical Anchors, in *Proceedings of the 1st International Geotechnical Symposium on Helical Foundations*, pp. 211–224.

McDowell, G. R., Falagush, O. and Yu, H.-S. (2012) A particle refinement method for simulating DEM of cone penetration testing in granular materials, *Géotechnique Letters*. Thomas Telford Ltd, 2(3), pp. 141–147. doi: 10.1680/geolett.12.00036.

Nguyen, T. T. V., Matsumura, S. and Kawamura, S. (2020) Model test and DEM investigations into effects of cavities on a single pile in weak rock, *Géotechnique Letters*, 10(2), pp. 216–226. doi: 10.1680/jgele.19.00004.

Previtali, M., Ciantia, M. O., Spadea, S., Castellanza, R. and Crosta, G. (2021) Discrete Element Modeling of Compound Rockfall Fence Nets, in *International Conference of the International Association for Computer Methods and Advances in Geomechanics*, pp. 560–567. doi: 10.1007/978-3-030-64518-2_66.

Sharif, Y., Brown, M. J., Ciantia, M., Knappett, J., Davidson, C., Cerfontaine, B., Robinson, S. and Ball, J. (2019a) Numerically Modelling the Installtion and loading of Screw Piles using DEM, in Davidson, C. ;, Brown, M. J., Knappett, J. A., Brennan, A. J., Augarde, C. E., Coombs, W. M., Wang, L., Richards, D., White, D. J., and Blake, A. (eds) *International Symposium on Screw Piles for Energy Applications*. Dundee, UK: University of Dundee, pp. 101–108. doi: 10.20933/100001123.

Sharif, Y., Ciantia, M., Brown, M. J., Knappett, J. A. and Ball, J. D. (2019b) Numerical Techniques For the Fast Generation of Samples Using the Particle Refinement Method, in *Proceedings of the 8th International Conference on Discrete Element Methods*. Enschede, Netherlands, p. 181.

Sharif, Y. U., Brown, M. J., Cerfontaine, B., Davidson, C., Ciantia, M. O., Knappett, J., Ball, J. D., Brennan, A. J., Augarde, C. E., Coombs, W., Blake, A., Richards, D., White, D., Huisman, M. and Ottolini, M. (2021) Effects of screw pile installation on installation requirements and in-service performance using the Discrete Element Method, *Canadian Geotechnical Journal*, 58(9), pp. 1334–1350. doi: 10.1139/cgj-2020-0241.

Zhang, N., Arroyo, M., Ciantia, M. O. and Gens, A. (2021) Energy balance analyses during Standard Penetration Tests in a virtual calibration chamber, *Computers and Geotechnics*, 133, p. 104040. doi: 10.1016/j.compgeo.2021.104040.

Table captions

Table 1: HST95 sand physical and numerical properties (Sharif et al. 2019a)

Table 2: Soil bed or bed properties

Table 3: Time required to run each phase of the DEM simulations.

Figure captions

Figure 1: a) Comparison of CPT cone resistance with depth for field tests and the DEM simulations b) Comparison of calculated relative density with depth for field tests and the DEM simulations

Figure 1: Schematic diagram of screw piles used in the DEM simulations; all screw piles are 3m in length (as was the case in the field study)

Figure 2: Schematic plan of pile load test locations in relation to CPT shown in Figure 1

Figure 4: Image of soil DEM bed created using the particle refinement method, a) plan view of Particle scaling in concentric zones b) Partially installed screw pile with 3 inch (76.2 mm) helix pitch. (colour of particles indicates the regions of different particle scale, density layering not shown for clarity) c) Close up of particles surrounding the 3 inch (76.2 mm) helix

Figure 5: Advancement ratio with depth from field measurements, replicated during the installation in DEM of each pile

Figure 6: Installation torque with depth for screw piles of various helix pitches from DEM and field tests

Figure 7: Uplift capacity against normalised displacement for screw piles of various helix pitches from DEM and field tests

Figure 8: Back calculated empirical torque correlation factor of screw piles used in this paper.

Notation list

BGL	Below ground level
CPT	Cone penetration test
DEM	Discrete element method
AR	Advancement ratio
D_{30}	soil particle diameter at which 30% of the mass of a soil specimen is finer
D_{60}	soil particle diameter at which 60% of the mass of a soil specimen is finer
D_c	core diameter
D_h	Helix diameter
D_R	Relative density
G	Shear Modulus
K_t	Torque correlation factor
q_c	CPT cone resistance
Q_t	Tensile capacity
T	Installation torque
γ	Sand unit weight
γ_{max}	Maximum dry density
γ_{min}	Minimum dry density
δ	Interface friction angle
μ	Friction coefficient
μ_{pile}	Interface friction coefficient
ν	Poissons ratio
φ	Critical state frictional angle

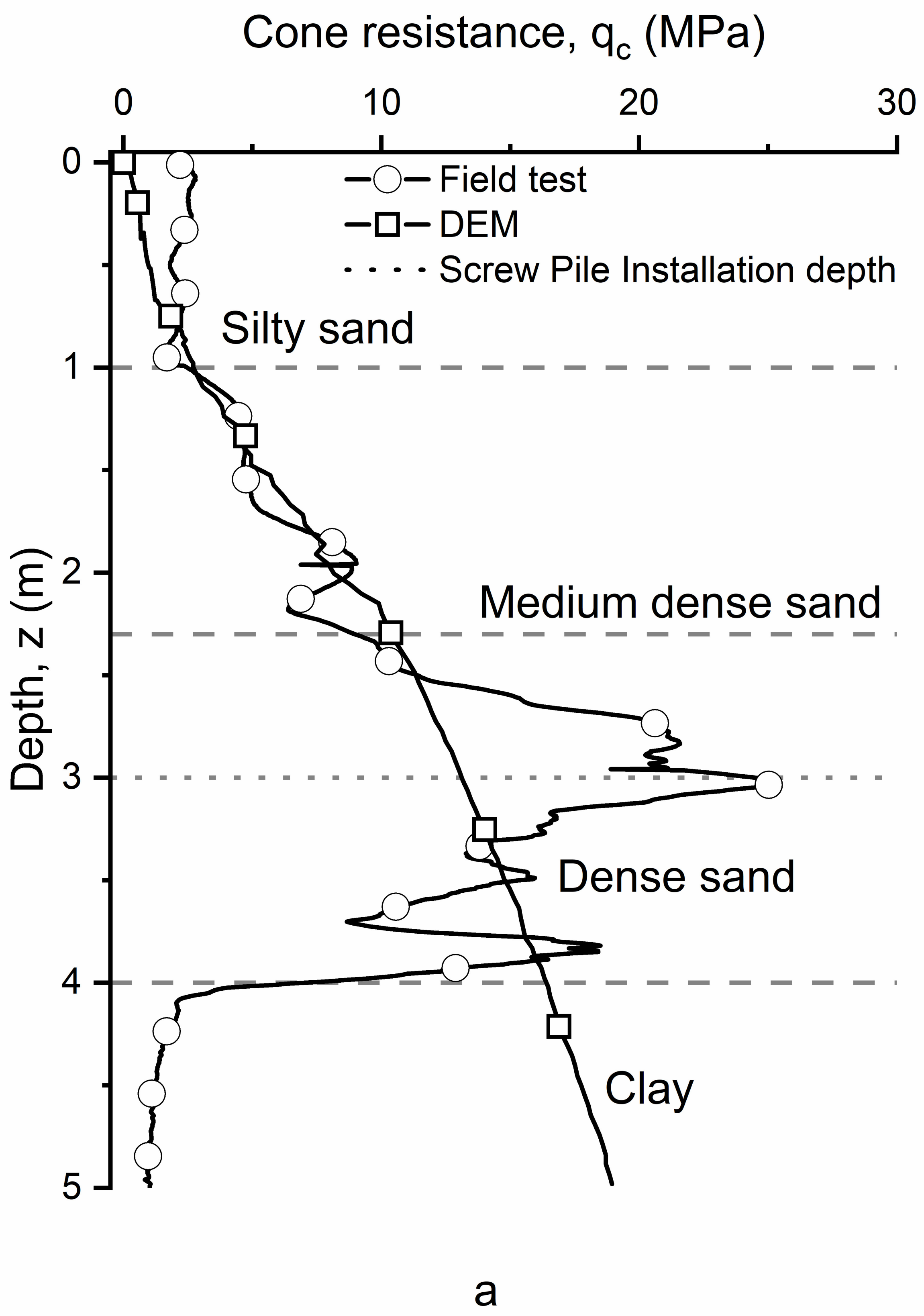
Cone resistance, q_c (MPa)
0
10
20
30
Depth, z (m)
0
1
2
3
4
5
Field test
DEM
Screw Pile Installation depth
Silty sand
Medium dense sand
Dense sand
Clay
a

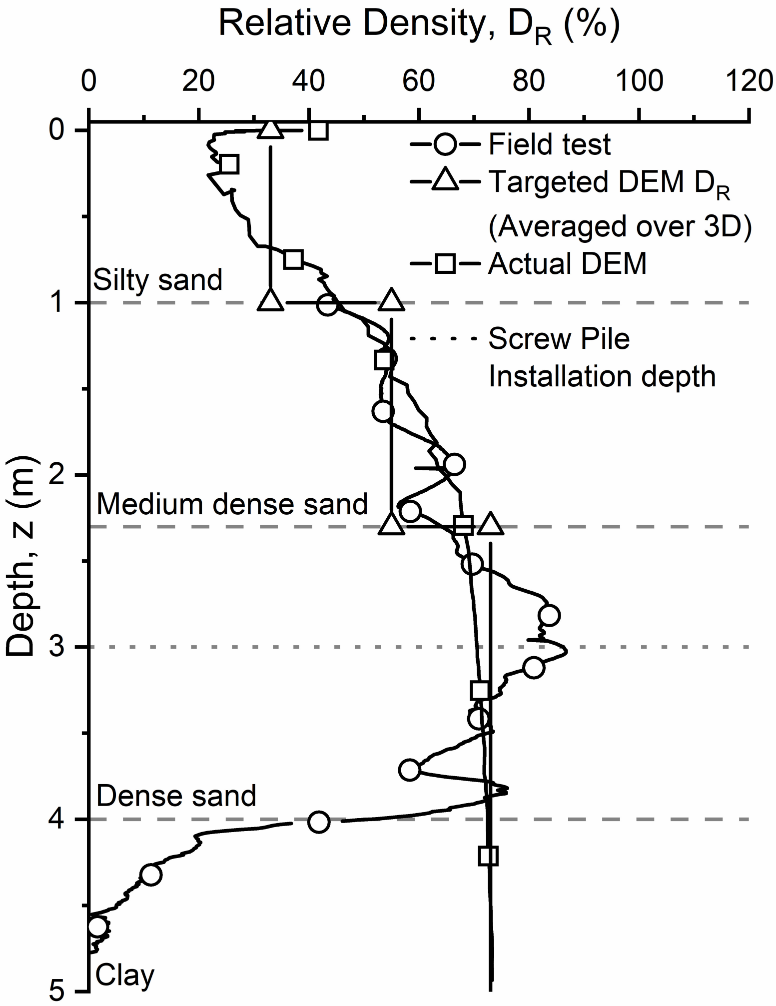
Relative Density, D_R (%)
0
20
40
60
80
100
120
Depth, z (m)
0
1
2
3
4
5
Field test
Targeted DEM D_R
(Averaged over 3D)
Actual DEM
Screw Pile
Installation depth
Silty sand
Medium dense sand
Dense sand
Clay

b

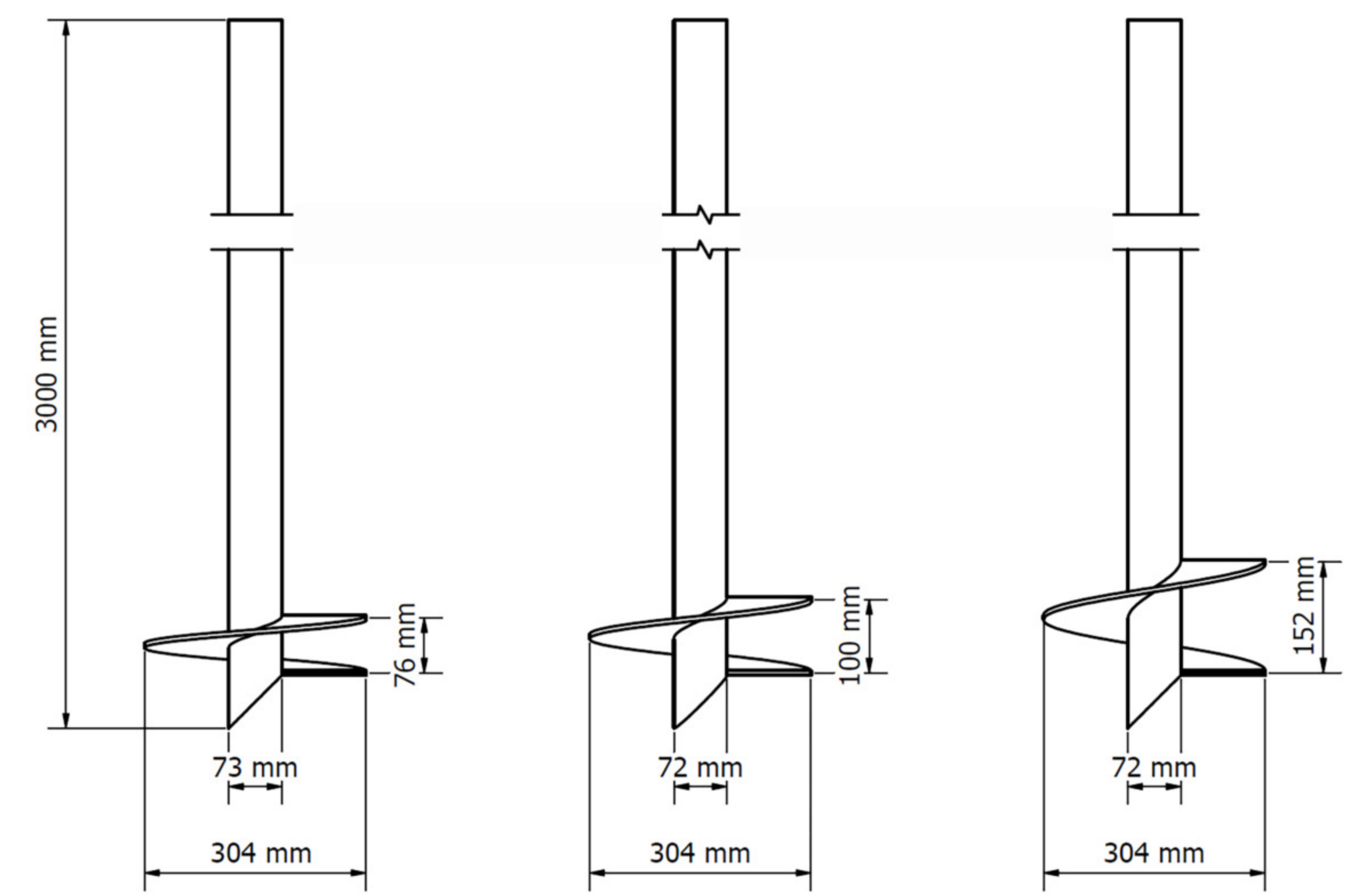
3000 mm
76 mm
73 mm
304 mm
100 mm
72 mm
304 mm
152 mm
72 mm
304 mm

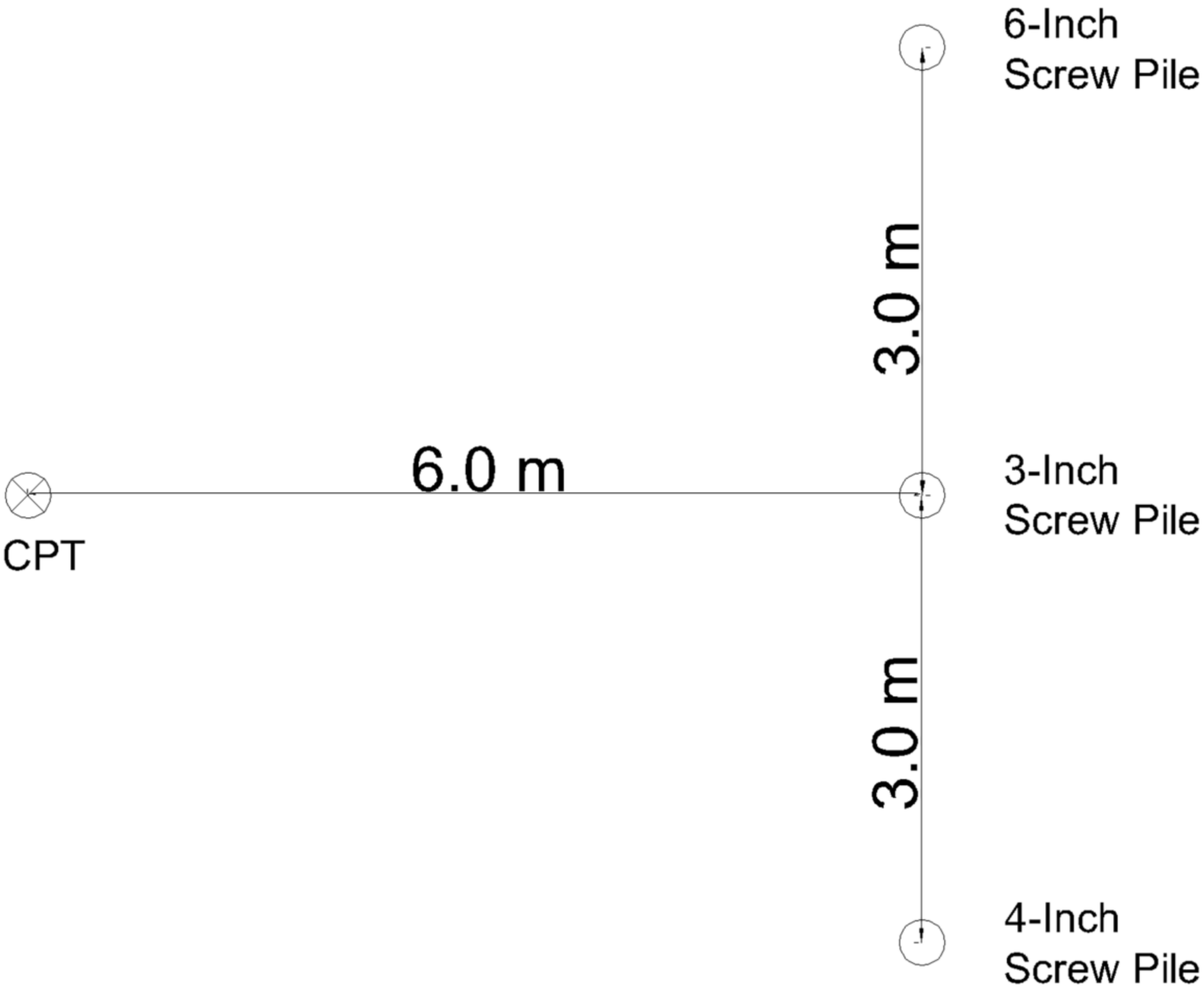
6-Inch
Screw Pile
3.0 m
6.0 m
3-Inch
Screw Pile
CPT
3.0 m
4-Inch
Screw Pile

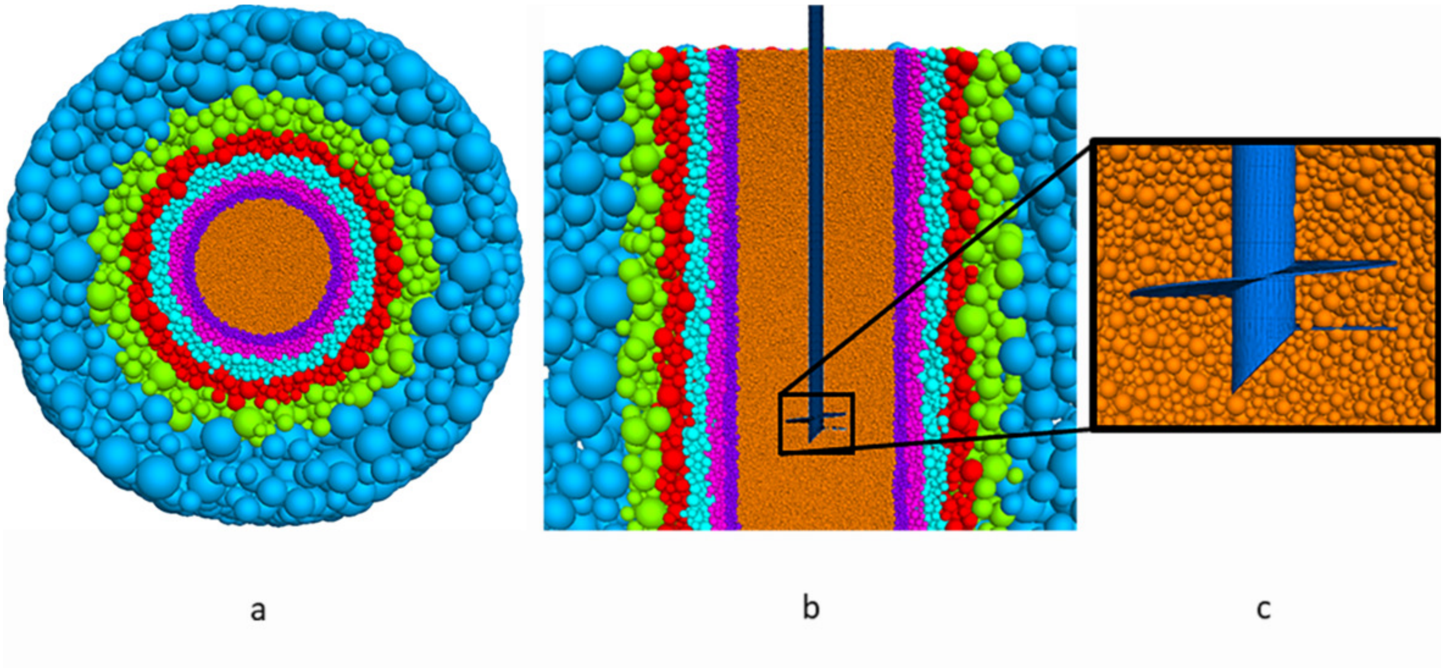
a
b
c

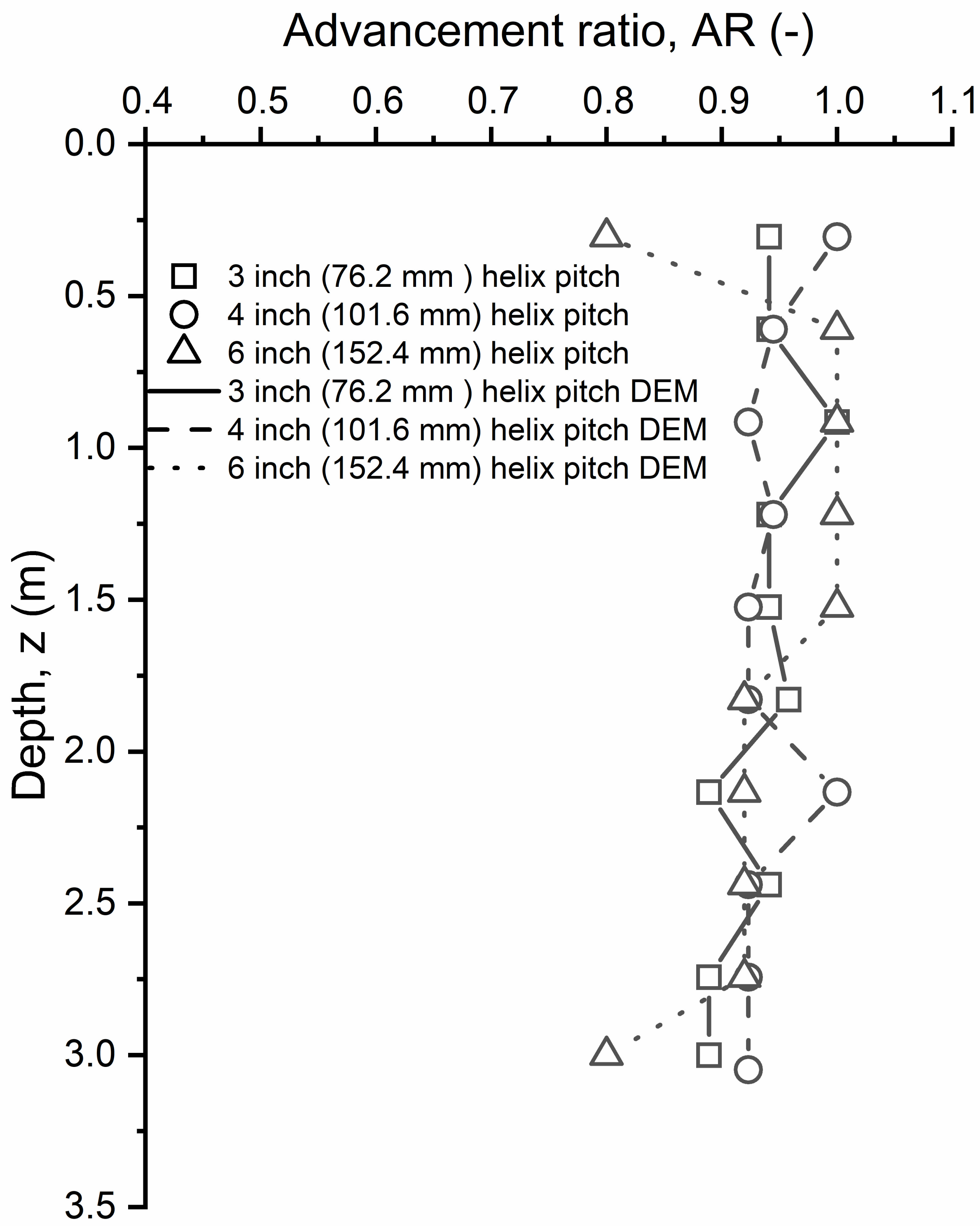
Advancement ratio, AR (-)
0.4
0.5
0.6
0.7
0.8
0.9
1.0
1.1
Depth, z (m)
0.0
0.5
1.0
1.5
2.0
2.5
3.0
3.5
3 inch (76.2 mm) helix pitch
4 inch (101.6 mm) helix pitch
6 inch (152.4 mm) helix pitch
3 inch (76.2 mm) helix pitch DEM
4 inch (101.6 mm) helix pitch DEM
6 inch (152.4 mm) helix pitch DEM

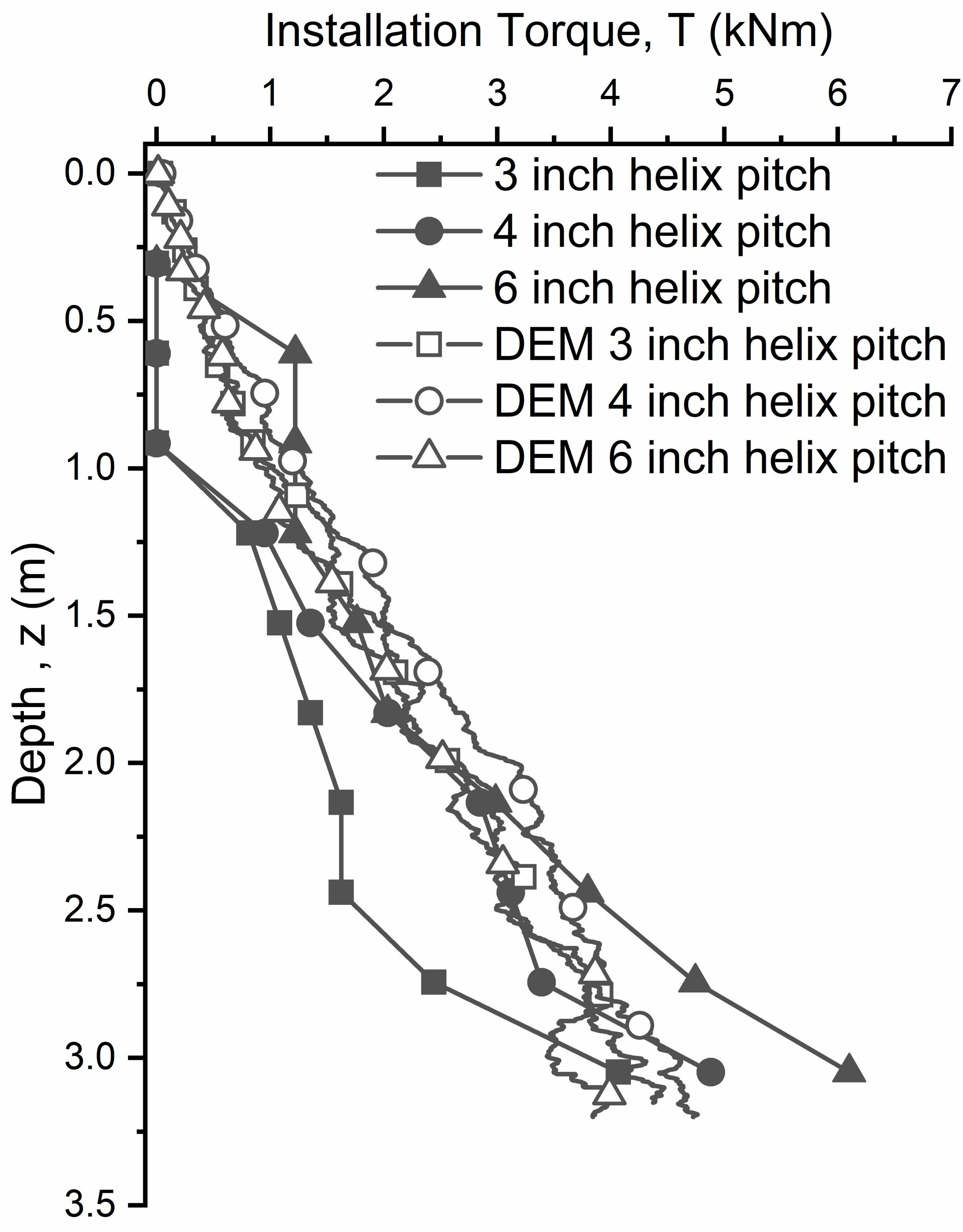
Installation Torque, T (kNm)
0 1 2 3 4 5 6 7
0.0 0.5 1.0 1.5 2.0 2.5 3.0 3.5
Depth , z (m)
3 inch helix pitch
4 inch helix pitch
6 inch helix pitch
DEM 3 inch helix pitch
DEM 4 inch helix pitch
DEM 6 inch helix pitch

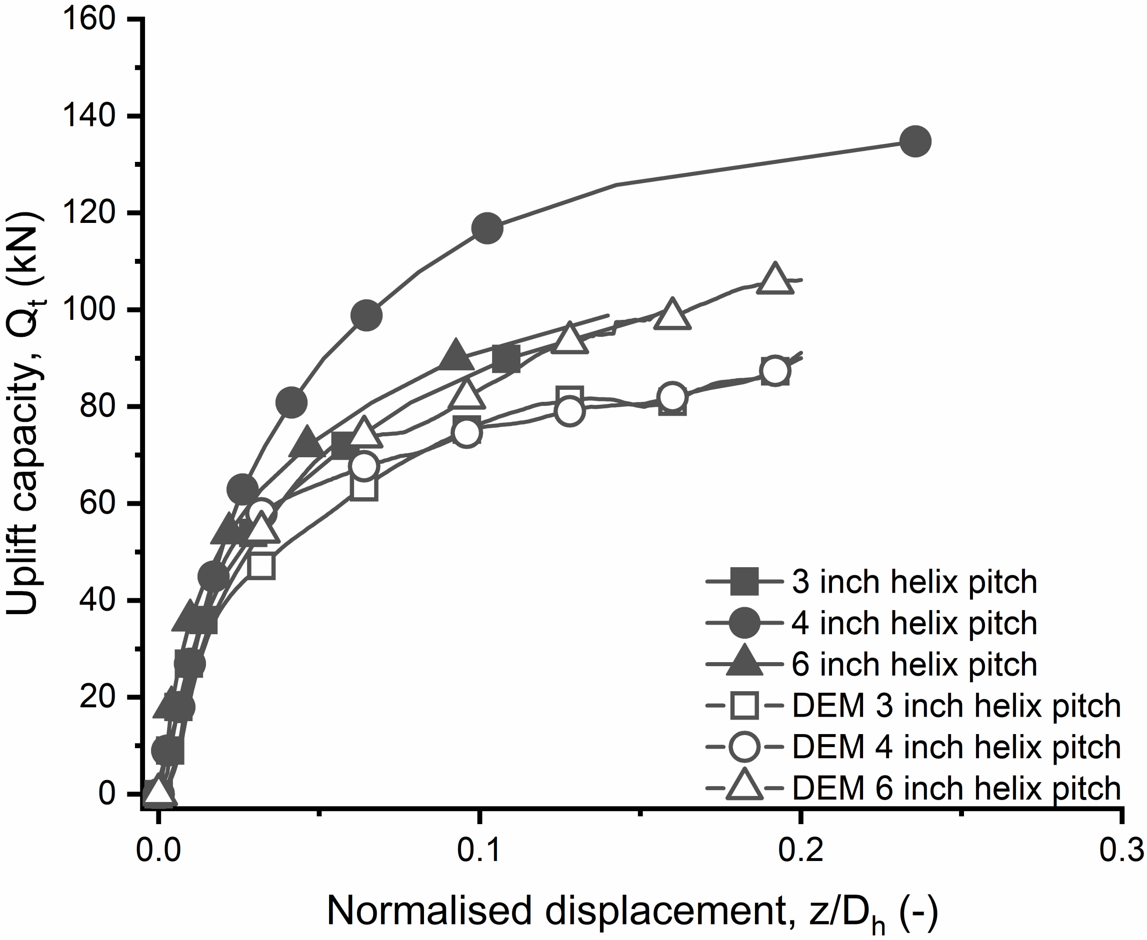

Uplift capacity, Q_t (kN)
160
140
120
100
80
60
40
20
0
0.0
0.1
0.2
0.3
Normalised displacement, z/D_h (-)
3 inch helix pitch
4 inch helix pitch
6 inch helix pitch
DEM 3 inch helix pitch
DEM 4 inch helix pitch
DEM 6 inch helix pitch

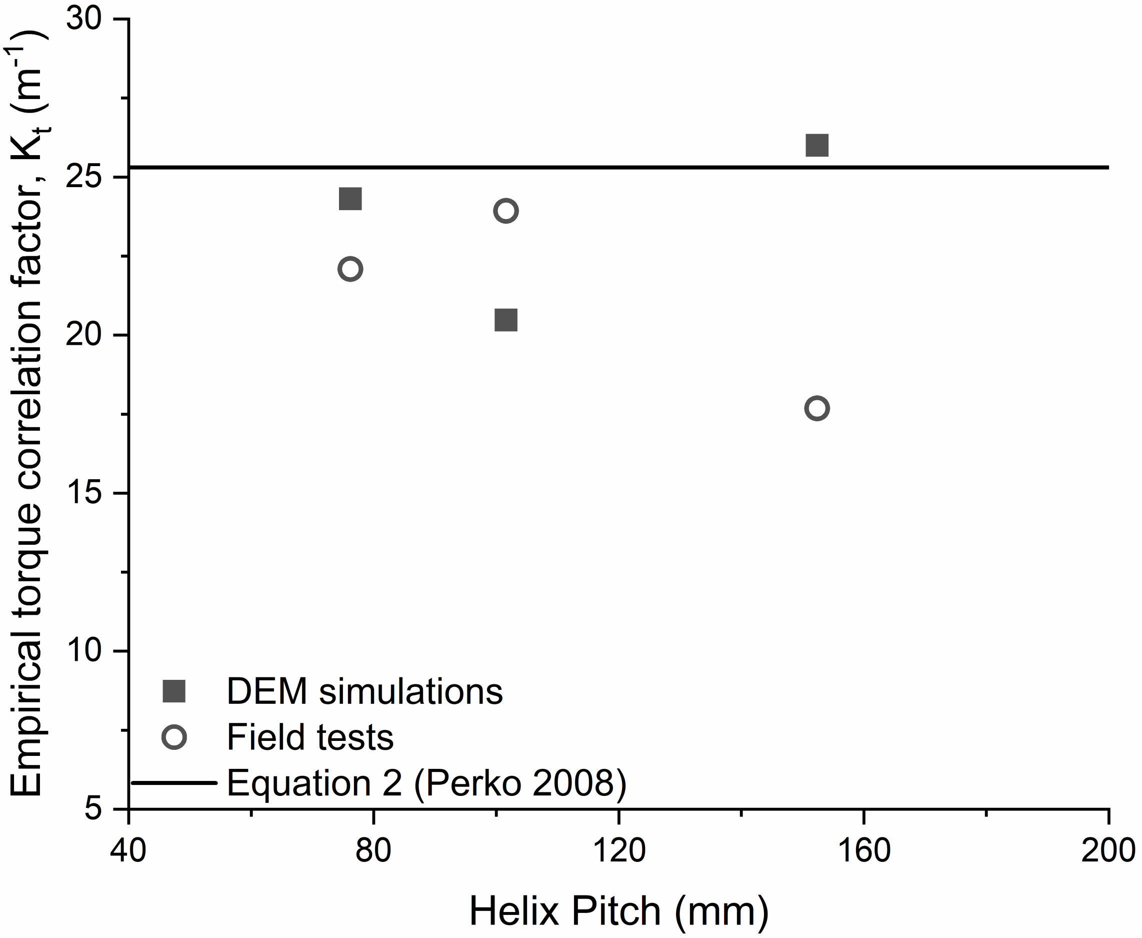
Empirical torque correlation factor, K_t (m^{-1})
30
25
20
15
10
5
40
80
120
160
200
Helix Pitch (mm)
DEM simulations
Field tests
Equation 2 (Perko 2008)

Table 1: HST95 sand physical and numerical properties (Sharif et al. 2019a)

HST95 silica sand property	Value
Physical properties	
Sand unit weight γ (kN/m^3)	16.75
Minimum dry density γ_{max} (kN/m^3)	14.59
Maximum dry density γ_{min} (kN/m^3)	17.58
Critical state friction angle, φ (degrees)	32
Interface friction angle, δ (degrees)	18
D_{30} (mm)	0.12
D_{60} (mm)	0.14
DEM Parameters	
Shear modulus, G (GPa)	9
Friction coefficient, μ (-)	0.264
Poisson's ratio, ν (-)	0.3
Interface friction coefficient [pile], μ_{pile} (-)	0.16

Note : No local nor global damping used in any of the simulations

Table 1: Soil bed or bed properties

Soil Bed property	**Value**
Total Height	6m
Diameter	3m
Layer 1 depth	0-1m
Layer 2 depth	1-2.3m
Layer 3 depth	2.3m-5m
Central zone PSD scaling	120
Total number of particles	850,000

Table 1: Time required to run each phase of the DEM simulations

Phases of the simulation	Time (h)
Layer 1 formation	12
Layer 2 formation	6
Layer 3 formation	11
Combining of layers	8
Installation of Pile	120
Uplift capacity test	5